High-Frequency Power Reflects Dual Intentions of Time and Movement for Active Brain-Computer Interface

Jiayuan Meng, Xiaoyu Li, Simiao Li, Xinan Fan, *Member, IEEE,* Minpeng Xu*, *Senior Member, IEEE,* and Dong Ming, *Senior Member, IEEE*

***Abstract*—Active brain-computer interface (BCI) provides a natural way for direct communications between the brain and devices. However, its detectable intention is very limited, let alone of detecting dual intentions from a single electroencephalography (EEG) feature. This study aims to develop time-based active BCI, and further investigate the feasibility of detecting time-movement dual intentions using a single EEG feature. A time-movement synchronization experiment was designed, which contained the intentions of both time (500 ms vs. 1000 ms) and movement (left vs. right). Behavioural and EEG data of 22 healthy participants were recorded and analyzed in both the before (BT) and after (AT) timing prediction training sessions. Consequently, compared to the BT sessions, AT sessions led to substantially smaller absolute deviation time behaviourally, along with larger high-frequency event-related desynchronization (ERD) in frontal-motor areas, and significantly improved decoding accuracy of time. Moreover, AT sessions achieved enhanced motor-related contralateral dominance of event-related potentials (ERP) and ERDs than the BT, which illustrated a synergistic relationship between the two intentions. The feature of 20–60 Hz power can simultaneously reflect the time and movement intentions, achieving a 73.27% averaged four-classification accuracy (500 ms-left vs. 500 ms-right vs. 1000 ms-left vs.1000 ms-right), with the highest up to 93.81%. The results initiatively verified the dual role of high-frequency (20–60 Hz) power in representing both the time and movement intentions. It not only broadens the detectable intentions of active BCI, but also enables it to read user's mind concurrently from two information dimensions.**

***Index Terms*—Active brain-computer interface, high-frequency power, single-interval timing prediction, movement, dual intention.**

I. Introduction

BRAIN-computer interface (BCI) is a rising technology that can provide a direct communication pathway between the brain and external devices, ingeniously integrating biological intelligence and machine intelligence. Electroencephalography (EEG) is the most commonly used signal for BCIs [1], [2]. According to signal generation mode, EEG-BCI can be divided into active, reactive and passive types [3]. In particular, the active BCI uses EEG signals that are independent of external stimuli and can directly reflect users' target intention, making BCI controls closer to the natural expression of brain intention. However, at present, active BCIs primarily rely on movement-induced event-related desynchronization/synchronization (ERD/ERS) [4], [5], the limited control signal restricts the detection of diverse intentions and severely hindered active BCIs from working in more application scenarios. Therefore, it is of vital importance to adapt additional voluntary mental activities into an active BCI, expanding the intentions that can be detected by active BCI.

Time is a fundamental dimension of our existence; it is a ubiquitous experience and a building block for effective perceptions and actions. During almost all the daily interactions between brain and external environment, target time intentions are often expressed by actively estimating the onset moment of upcoming events, which is also known as timing prediction [6], [7]. Therefore, active BCI is promising to make a great progress if the time intention can be successfully detected. To achieve this, it is necessary to thoroughly investigate effective EEG encoding and decoding of timing prediction. There are two ways for generating timing prediction, i.e., beat-based rhythmic or memory-based single-interval timing prediction [8], [9], [10]. Evidently, the latter is much closer to user's mindset and more widely used, despite that its available neural evidence is much less than the rhythmic one and harder to encode. Previous studies suggest that the contingent negative variation, N1-P2/N2 and P300 are modulated by single-interval timing [11], [12], [13], [14]. Recent studies propose that neural oscillations are instrumental in the preparation or maintenance of time

This work was supported by the STI 2030—Major Projects (Grant No. 2022ZD0208900); National Natural Science Foundation of China (No. 81925020, 62106173, 82330064, 62122059); General Projects of Postdoctoral Science Foundation of China (2022M712364); Tianjin Natural Science Foundation (22JCYBJC01480); China Aerospace Science and Industry Brain Computer Innovation Center 2023 "Aviation Brain" Young Scholars Fund. (**Corresponding author: Minpeng Xu*).
Jiayuan Meng and Xiaoyu Li contributed equally to this work.

Xiaoyu Li, Simiao Li are with the Academy of Medical Engineering and Translational Medicine, Tianjin University, Tianjin 300072, China.

Jiayuan Meng, Minpeng Xu, and Dong Ming are with the Academy of Medical Engineering and Translational Medicine, Tianjin University, Tianjin 300072, China, and also with the Haihe Laboratory of Brain–Computer Interaction and Human–Machine Integration, Tianjin 300392 China. Xinan Fan is with Beijing Machine and Equipment Institute, Beijing, China. (e-mail: xmp52637@tju.edu.cn).

This work involved human subjects in its research. Approval of all ethical and experimental procedures and protocols was granted by the Institutional Review Board at Tianjin University under Application No. TJUE-2021-055.

information [15], [16]. Our prior research further established that single-interval timing prediction with varied length, i.e., 400 ms vs. 600 ms, led to distinct beta-gamma ERDs and sequential delta event-related potential (ERP) enhancement [17], [18]. These features were verified to be separable, preliminarily confirming the feasibility of detecting time intention.

Movement and timing prediction are believed to share certain neural structures and mechanisms [19], [20], [21], with some timing prediction studies even reported similar alpha, beta or gamma oscillation patterns as those of movement [22], [23], [24]. This finding suggests the potential for simultaneous detection of time and movement from a single EEG feature. This dual detection capability in active BCI could enhance precision and reduce delay, enabling not only spatial but also temporal awareness. However, existing encoding and decoding knowledge is far from enough to realize perfect time-movement dual detection. Most important of all, it remains unknown whether the two intentions essentially work in a synergistic or interinhibitive way. Previous studies reported the unidirectional facilitation effect of one intention on the other [25], [26], [27], [28], but none paid equal attention to neural responses of both time and movement, leaving a confusion of whether one intention would be influenced when the other is enhanced. What's more, the memory-based single-interval timing prediction widely used in interaction tends to trigger more endogenous signals and taking up more cognitive resources than the beat-based rhythmic one mentioned in the above studies [29], [30], which may encroach on the resources for motor expression. Therefore, it is necessary to address a complementary question. What's the interaction pattern between movement and precise single-interval timing prediction? We hypothesize that there exists a single EEG feature that effectively reflects both intentions.

This study designed a trainable time-movement synchronization experiment that can concurrently encode the intentions of time (500 ms vs. 1000 ms) (supplementary A.1) and movement (left vs. right). The experiment was conducted in both the before (BT) and after (AT) training sessions, which aims to explore whether precise timing prediction is an innate talent or can only be obtained from training, and investigate whether movement intention could remain robust when timing prediction is enhanced. The behavioural and EEG data from the pre-movement period were analyzed. As a result, AT sessions led to evidently increased time-related high-frequency (30–60 Hz) ERD in frontal-motor areas, along with strengthened motor-related contralateral dominance of ERP and 20–30 Hz ERD, which confirmed the beneficial role of training in improving timing prediction precision, preliminarily verified the feasibility of time-movement dual encoding. The decoding result based on a single EEG feature, i.e., 20–60 Hz power, achieved 65.18% and 73.27% averaged four-classification accuracy for the BT and AT sessions, respectively, with the highest four-classification accuracy of 93.81%. This study provides a completely new approach for multidimensional information detection of active BCI, and provides more neural evidence for better understanding the interactions between time and movement.

II. Method

A. Participants

Twenty-two healthy volunteers (15 females, 19–25 years old), who were students in Tianjin University, participated in this study. All participants were right-handed and had normal or corrected-to-normal vision. They were all free from psychological or neurological diseases and had sufficient rest before the experimental procedures. Experimental procedures involving human volunteers were approved by the Institutional Review Board at Tianjin University. All possible consequences of the experiment were explained, and written informed consent was obtained from each participant.

B. Experimental procedures

A time-movement synchronization experiment was designed for this study. Auditory and visual stimuli of this experiment were generated by the MATLAB Psychtoolbox toolkit and presented on a 27-inch LED screen placed 80 cm away from the subject at eye level. To better understand the differences between the conditions with and without precise timing prediction, a training process was involved, and the formal experiments were conducted in both BT and AT sessions. Generally, the training process after the formal BT experiment took about three days, and the formal AT experiment was conducted on the day immediately after training process.

Fig. 1(a) and (b) shows the detailed process of the single-trial formal BT and AT experiments. Specifically, each trial started with a 1000 ms audio-visual cue to inform subjects of the required length of the following single-interval timing by cue colors (white: 500 ms; blue: 1000 ms). Then there was a blank period with a duration of 1000–2000 ms at random. After that, the first flash emerged and lasted for 120 ms. When it disappeared, subjects began to timing and indicated the end of a specific time period by pressing the button. Feedback indicating the deviation time, which was the difference between subjective and standard timing, appeared 100 ms after the button press. At last, there was a random blank period of 1000 to 1500 ms. There were 8 blocks in each experiment, and each block contained 30 trials. The 500 ms and 1000 ms timing tasks were carried out randomly with equal probability. Moreover, subjects were instructed to press the button using their right index in four blocks and their left index in the other four blocks. All the blocks were presented randomly. Therefore, such process can form four time-movement conditions, i.e., 500 ms-right, 500 ms-left, 1000 ms-right, 1000 ms-left, each condition has 60 trials.

The training process included two parts. The first part mainly showed participants with the standard 500 ms/1000 ms time interval in order to enhance subjects' precise timing ability. The second part was consistent with formal experiment, but only behavioural data was recorded. In the behavioural analysis,

This article has been accepted for publication in IEEE Transactions on Neural Systems and Rehabilitation Engineering. This is the author's version which has not been fully edited and content may change prior to final publication. Citation information: DOI 10.1109/TNSRE.2025.3529997

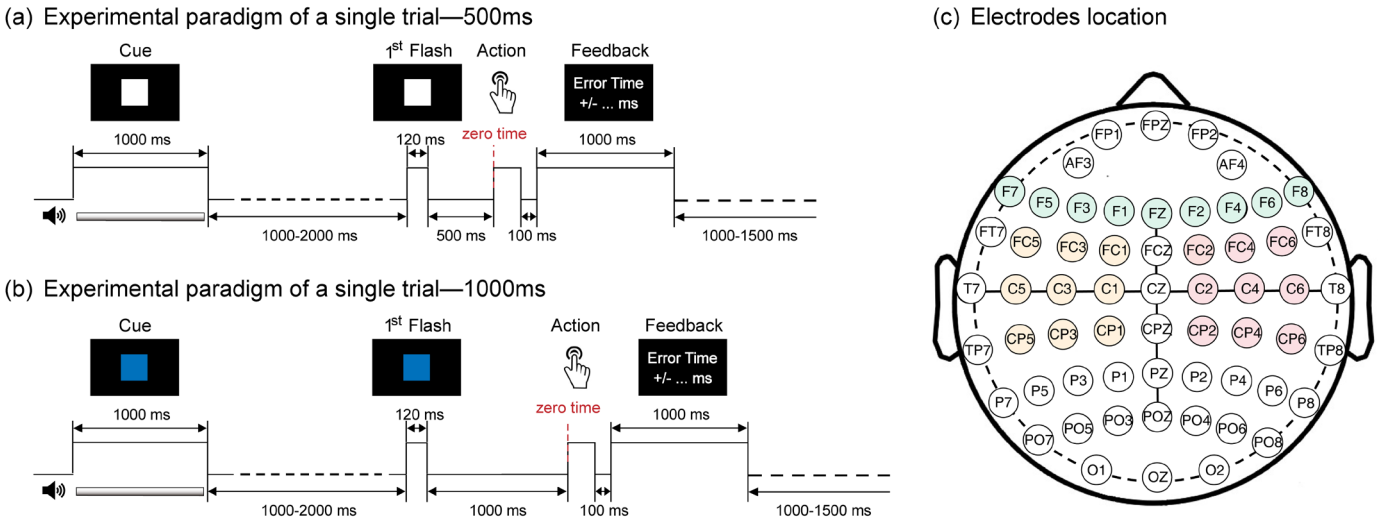

Fig. 1. Detailed procedure for a single trial. (a) Visual cues are presented in white for the 500 ms condition. (b) Visual cues are presented in blue for the 1000 ms condition. (c) The location of the electrodes.

trials with a deviation time within ±80 ms were defined as qualified trials, and behavioural accuracy was defined as the ratio of qualified trials to all trials. Subjects would not be allowed to start the AT formal experiment until the behavioural accuracy reached more than 80%.

The comparisons between BT and AT can reflect how neural representation changed with improved timing precision, as well as provide an approach for investigating the impact of the introduction of time information on the encoding and decoding of movement intention. Fig. 1(c) shows the exact location of the electrodes, with green, yellow and pink representing the frontal area, left motor area and right motor area, respectively.

C. EEG data acquisition and pre-processing

Scalp EEG signals were recorded by the Neurocan Synamps2 system at a sampling rate of 5000 Hz. EEG data of 64 electrodes were collected by Quik Cap electrode cap according to the international 10–20 system. The reference electrode was set on the top of the head and grounded to the forehead, and the notch frequency was set at 50 Hz. In the pre-processing process, the stored EEG data was down-sampled to 500 Hz by using MATLAB's EEGLAB toolkit, and the signal was band-pass filtered by 0.1–100 Hz by FIR I band-pass filter. The data from -1500 ms to 1000 ms relative to the button press (i.e., 0 ms) was selected for further analysis. We selected the moment of button press as the zero time for consistent data alignment across all trials, ensuring that the period leading up to the button press captures both time and movement intentions.

D. EEG signal analysis

The ERP analysis was conducted, setting the average value from the time period of -1500 ms to -1300 ms before the button press as the baseline. The clustering-based permutation test in Fieldtrip was used to statistics each time point, and ultimately selecting -500–0 ms as the expected time window for both 500 ms and 1000 ms ERP component analysis.

The event-related spectral perturbation (ERSP) was employed to investigate the event-related changes in spectral power over time across a broad frequency range. The spectral power values were computed using short-time Fourier transform on 1,250 data points within the time range of -1500 ms to 1000 ms, with a frequency resolution of 1.95 Hz. To examine the pre-movement ERD, the time window from -1500 ms to -1300 ms was used as the baseline.

Supported $F_i(f,t)$ was the spectral estimation of trials i EEG signals $x(t)$, where f represents frequency, t represents time, and N represents the number of trials. The ERSP was shown as equation:

$$ERSP(f,t) = \frac{1}{N}\sum_{i=1}^{k}\left(F_i(f,t)\right)^2 \quad (1)$$

Considering the time-frequency distribution characteristics of the ERSP (beta: 20–30 Hz; gamma: 30–60 Hz). Select -500–0 ms, 20–30 Hz (500 ms); -1000–0 ms, 20–30 Hz (1000 ms) as the time-frequency windows for studying movement information, and select -500–0 ms, 30–60 Hz (500 ms); -1000–0 ms, 30–60 Hz (1000 ms) as the time-frequency window for studying time information. Finally, it was found that 20–60Hz, -900–0 ms can be used for studying the time-movement dual intentions.

It is worth noting that the ERP, ERSP and their brain topographies were superimposed and averaged across all subjects.

E. EEG signal classification

Classification methods based on Riemannian geometry have proven to be highly effective in decoding power features. Within these methods, the primary concept of the Riemannian tangent space lies not in constructing a spatial filter, but rather

in directly mapping the data to a geometric space that is suitable for the metric analysis. Specifically, the covariance matrix present in the Riemannian manifold is mapped to a Euclidean space, enabling the utilization of various classification algorithms, including support vector machines (SVM), linear discriminant analysis (LDA), or logistic regression.

However, when dealing with EEG data, since the covariance matrices representing the multi-channel EEG signals are symmetric positive definite matrices (SPD) belonging to Riemannian manifolds, and most classification models are designed to operate within Euclidean spaces. Therefore, it becomes necessary to perform a tangent space mapping on all covariance matrices at a selected reference point.

Suppose $C_i \in R^{M\times N_C\times N_t}$ represents the covariance matrix, where M,N_C,N_t denote the trials, channels, and time points, respectively. Within this Riemannian manifold space, the shortest path from C_1 to C_2 is referred to as a geodesic. The distance along this geodesic can be calculated using the following equation:

$$\delta_R(C_1, C_2) = [\sum_{n=1}^{N} log^2\, \lambda_n]^{\frac{1}{2}} \quad (2)$$

where λ_n denotes the n_{th} eigenvalue of $C_1^{-1}C_2$.

In the Riemannian manifold, the symmetric positive definite matrix, denoted as M, that minimizes the sum of squared Riemannian distances to each covariance matrix, is considered the Riemannian mean of the covariance matrices.

$$M = \underset{C\epsilon SPD}{\operatorname{argmin}} \sum_{i=1}^{I} \delta_R^2\,(C, C_i) \quad (3)$$

In equation, I represents the number of covariance matrices on the manifold, and SPD represents the set of symmetric positive definite matrices of the same dimension.

Mapping each covariance to the tangent vector in the Riemannian tangent space is typically done by choosing the Riemannian mean M as the reference point, at this point:

$$S_i = log_M(C_i) = M^{1/2}\ log(\,M^{-1/2}C_i\,M^{-1/2})M^{1/2} \quad (4)$$

$$s_i = upper(\,M^{-1/2}S_i\,M^{-1/2}) \quad (5)$$

The symbol s_i in the above equation represents the tangent vector obtained by mapping C_i to the tangent space with the Riemannian mean M as the reference point.

After mapping the covariance matrices on the Riemannian manifold to tangent vectors, the logistic regression classification (LogR) model is applied through the tangent vectors to complete the classification and prediction, abbreviated as the tangent space logistic regression algorithm (TS+LogR). The data used for classification is three-dimensional data $X_K \in R^{M\times N_C\times N_t}$. The data length ranges from -900 ms to 0 ms (supplementary A.2), with a total of 450 data points. The classification is performed using all 60 channels and ten-fold cross-validation to calculate the classification accuracy. Additionally, based on the ERSP results, the 20–30 Hz and 30–60 Hz are first selected for decoding movement and time intention, respectively. Finally, 20–60 Hz, which is demonstrated have higher motor classification accuracy than the 20–30 Hz, is selected for decoding the time-movement dual intentions.

F. Statistical analysis

Statistical analyses were first conducted on behavioural results using a two-way repeated measures ANOVA. The factor of movement (left vs. right) and timing-prediction-related training (BT vs. AT) was defined as the within-subject and between-subject factor, respectively.

As to statistical analyses of EEG data, to test the interactions between movement and training of timing prediction, a two-way repeated measures ANOVA was performed, defining movement (left vs. right) and timing-prediction-related training (BT vs. AT) as the within-subject and between-subject factor, respectively. In cases where the interactive effect was presented, further analyses were conducted to explore the separate effects of each factor. Conversely, if no interactive effect was found, the main effects of timing-prediction-related training and movement were examined. In addition, to evaluate whether timing-prediction-related training have an impact on the EEG responses of timing prediction, paired sample t-tests were conducted on the time-related EEG responses between BT and AT session. The time-related classification also utilized a paired sample t-test to compare differences between BT and AT session.

Error bars represented standard deviation, and Bonferroni correction was applied to all the conditions accounting for multiple comparisons. Statistical significance was determined based on a p-value threshold of less than 0.05. All statistical analyses were conducted using the SPSS software package.

III. Result

A. Behavioural analyses

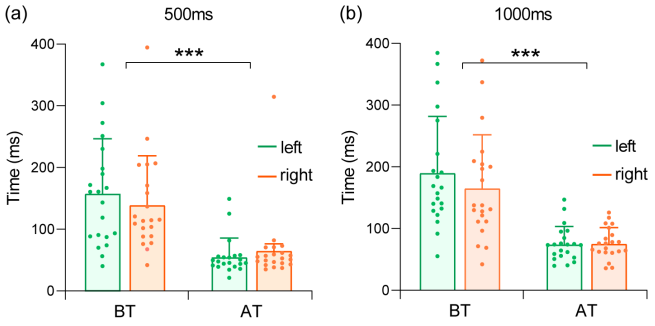

Fig. 2. Comparative analysis of absolute deviation time in BT and AT sessions. (a) Under the 500 ms condition. (b) Under the 1000 ms condition. Abbreviation: BT-Before training; AT-After training (The following text is the same as it). ***: P<0.001

In behavioural analyses, the absolute deviation time, i.e., the absolute value of the difference between subjective timing and standard time interval, was calculated under the 500 ms and 1000 ms conditions, respectively. Fig. 2 (a) shows that in the 500 ms condition, the absolute deviation time was 158.85± 87.83 ms (left), 140.13±78.92 ms (right) in BT sessions, and

55.87±29.67 ms (left), 66.23±12.86 ms (right) in AT sessions. Fig. 2 (b) shows in the 1000 ms condition, absolute deviation time was 191.11±90.76 ms (left) and 166.31±85.54 ms (right) in BT sessions, 75.29±28.12 ms (left) and 76.47±25.06 ms (right) in AT sessions. In both conditions, absolute deviation time was significantly reduced (500 ms: $F(1,21)=68.9$, $P<0.001$; 1000 ms: $F(1,21)=65.53$, $P<0.001$) and standard deviations became much smaller in AT sessions, which indicated the precise timing prediction was successfully built up in AT sessions. It is also evident that the left or right hand had almost no impact on the absolute deviation times (500 ms: $F(1,21)=0.067$, $P=0.79$; 1000 ms: $F(1,21)=0.8$, $P=0.38$). Moreover, compared to 500 ms, the 1000 ms condition had a much larger absolute deviation time in both BT and AT, consistent with previous findings reporting the accuracy of timing decreased as the temporal length prolonged [31].

B. ERP analyses

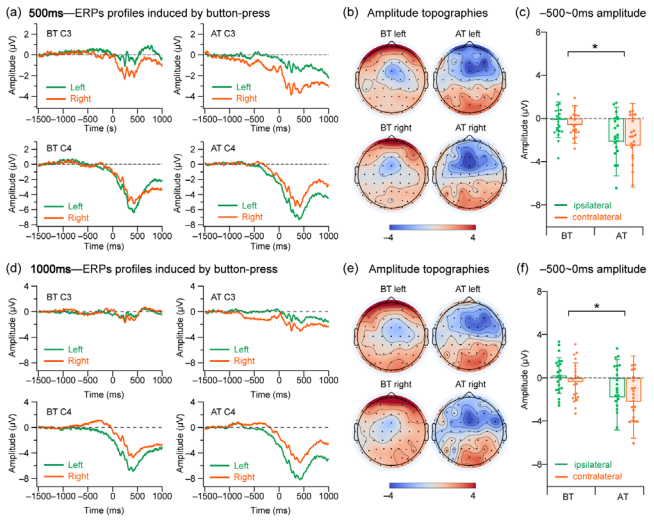

Fig. 3. (a) In the 500 ms condition, averaged ERPs evoked by left- and right-movement under C3 and C4 channels, respectively, zeros indicated button press moment. (b) Amplitude topographies. (c) Comparison of amplitudes in bilateral motor areas. (d) In the 1000 ms condition, averaged ERPs under C3 and C4 channels. (e) Amplitude topographies. (f) Amplitude comparison. *: 0.01<*P*<0.05

The ERP of C3 and C4, which are typical electrodes located at motor-related areas, were analyzed to investigate whether the motor-related ERP still works after the involvement of precise timing prediction. As Fig. 3 (a, c) show, in the 500 ms condition, compared to the BT, AT sessions revealed much larger negative slopes in pre-movement (-500–0 ms) period ($F(1,21)=7.108$, $P=0.014$), showing a trend towards a motor-related contralateral dominance pattern. Fig. 3 (b) shows averaged amplitude topographies in pre-movement (-500–0 ms) period, more negative ERPs were found in contralateral brain areas of movement in the BT and AT sessions. Moreover, in AT sessions, the negative amplitude not only became much larger in motor areas, but also emerged in frontal areas (supplementary A.3).

As Fig. 3 (d–f) show, in the 1000 ms condition, there were similar motor-related ERP variations as 500 ms condition, and the involvement of precise timing prediction increased the amplitudes of negative ERPs ($F(1,21)=6.542$, $P=0.018$) and the tendency of motor-related contralateral dominance patterns, as well as expanding the range of activated brain regions, with significant negative ERPs likewise observed in frontal and motor regions. The results indicate that the motor-related ERP variations still exist and may be even larger after the involvement of precise timing prediction, providing the potential to simultaneously detect the time and movement intentions.

C. ERSP analyses

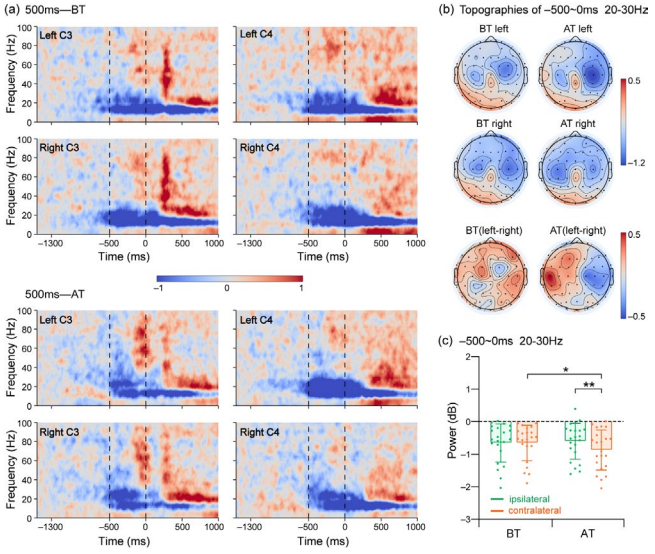

Fig. 4. (a) In the 500 ms condition, averaged ERSP time-frequency distribution under C3 and C4 in BT (upper) and AT (lower) sessions. (b) Topographic maps of averaged power within 20–30 Hz, -500–0 ms. (c) Statistical analysis of averaged power in bilateral motor areas. *: 0.01<*P*<0.05, **: 0.001<*P*<0.01

Fig 4 (a) shows ERSP time-frequency distributions under the 500 ms condition in the BT (upper) and AT (lower) sessions. Notably, in the typical motor-related frequency (10–30 Hz), the ERDs were almost the same among conditions in 10–20 Hz (supplementary A.4), yet differences were found in 20–30 Hz frequency range. Thus, the following analyses mainly focused on the 20–30 Hz ERDs in -500–0 ms time window. As Fig. 4 (b) shows, in BT sessions, ERD was found in bilateral motor areas, the left-right difference was small. Whereas in the AT session (Fig 4 (b, c)), a motor-related contralateral dominance pattern, in which the ERD on the contralateral side of movement was much larger than that on the ipsilateral ($F(1,21)=8.48$, $P=0.001$), was observed in both the left- or right-movement conditions. Contralateral ERD in the AT session was much larger than that of BT ($F(1,21)=8.48$, $P=0.04$), revealing a discernible interplay between the establishment of precise timing prediction and movement. Moreover, topographies of ERD differences between left- and

right-movement revealed obviously opposite power distribution in the AT session, where right and left hemispheres showed power increase and decrease, respectively.

Similar motor-related ERSP variations were also found in the 1000 ms condition. In BT sessions (Fig. 5 (a) (upper), (b)), motor-related ERDs were found in bilateral motor areas and similar between left- and right-movement. In AT sessions (Fig. 5 (a) (lower), (c)), the ERD was significantly larger than that in the BT session ($F(1,21)=6.542$, $P=0.018$), with a significant contralateral dominance of 20–30 Hz ERD when the left index moved; the ERD difference between left and right also revealed opposite variation in bilateral hemispheres. These results indicated that the beta (20–30 Hz) ERD can still represent movement intention when time encoding was involved, and precise timing prediction can even enhance the motor-related power feature.

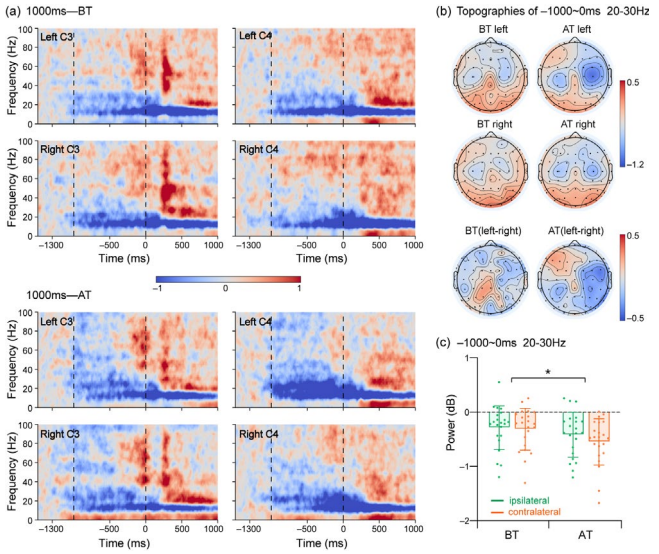

Fig. 5. (a) In the 1000 ms condition, averaged ERSP time-frequency distribution under C3 and C4 in BT (upper) and AT (lower) sessions. (b) Topographic maps of averaged power within 20–30 Hz, -1000–0 ms. (c) Statistical analysis of averaged power in bilateral motor areas. *: 0.01<*P*<0.05

The time-related ERSP features were then investigated. By comparing ERSP time-frequency distributions in Fig 4 (a) and 5 (a), we found noticeable ERD difference between the BT and AT sessions in the frequencies higher than 30 Hz, which may reflect a successful encoding of precise time information. Thus, the study investigated high-frequency (30–60 Hz) ERSP topographies. As shown in Fig. 6 (a, b), in the 500 ms condition, high-frequency ERD mainly located in the frontal-motor areas became much larger in the AT session (frontal: $T(21)=2.512$, $P=0.02$; motor: $T(21)=2.136$, $P=0.045$). In the 1000 ms condition (Fig. 6 (d, e)), AT session led to much larger the high-frequency ERD in motor areas ($T(21)=2.261$, $P=0.034$). Furthermore, this study explored the ERD difference between the 500 ms and 1000 ms conditions in Fig. 6 (c, f). Consequently, there was a significant difference between the two-timing predictions in AT sessions (left: $T(21)=-2.492$, $P=0.021$; right: $T(21)=-4.031$, $P=0.001$). The results indicated that high-frequency (30–60 Hz) ERD can reflect successful encodings of precise time information, and revealed distinctions between 500 ms and 1000 ms timing prediction.

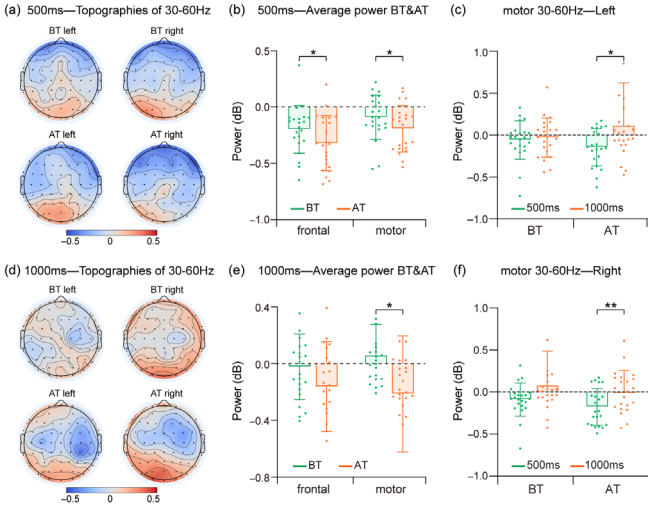

Fig. 6. (a) In the 500 ms condition, the topographic maps of 30–60 Hz, -1000–0 ms. (b) Averaged power analysis of the frontal and bilateral motor area. (c) Averaged power comparison under left hand. (d) In the 1000 ms condition, the topographic maps of 30–60 Hz, -1000–0 ms. (e) Averaged power analysis of the frontal and bilateral motor area. (f) Averaged power comparison under right hand. *: 0.01<*P*<0.05, **: 0.001<*P*<0.01

D. Decoding results of time-movement dual intentions

The ERSP analyses showed that 20–30 Hz and 30–60 Hz ERD have close associations with the movement and precise time information, respectively. Thus, it is necessary to further explore whether 20–60Hz ERD features could simultaneously decode time and movement dual information. TS+LogR method was used to calculate the classification accuracy in BT and AT sessions. As TABLE I shows, the classification accuracy of movement (left vs. right) was 98.20±5.80% and 97.47±9.17% in the BT and AT sessions, the establishment of precise timing prediction did not influence the detection of movement intentions ($T(21)=1.029$, $P=0.37$). The decoding performances of time intention (500 ms vs. 1000 ms) were then analyzed, yielding an averaged classification accuracy of 65.79 ±8.18% and 76.10±9.47%, respectively, for the BT and AT sessions. The establishment of precise timing prediction improved detection accuracy of time intention significantly ($T(21)=-4.038$, $P<0.001$). The decoding results of movement-time dual intentions (500 ms-left vs. 500 ms-right vs. 1000 ms-left vs. 1000 ms-right) showed that the averaged four-classification accuracy was 65.18±8.11% and 73.27±9.72% respectively for BT and AT sessions, with the highest four-class accuracy of 93.81%. The results not only indicated that the establishment of precise timing prediction can improve the decoding accuracy of time information ($T(21)=-3.992$, $P=0.001$), but also verified that the high-frequency power can simultaneously reflect the dual intentions of time and

movement.

TABLE I
THE CLASSIFICATION ACCURACY (%) FOR DATA WITH DIFFERENT CONDITIONS AT 20–60 HZ

Subject	Movement		Time		Dual intentions	
	BT	*AT*	*BT*	*AT*	*BT*	*AT*
S1	95.88	100.00	54.71	65.00	63.89	75.00
S2	100.00	99.44	66.67	79.44	61.67	67.92
S3	100.00	93.75	57.92	72.92	66.67	68.75
S4	100.00	99.58	61.25	74.58	75.56	91.67
S5	97.78	98.75	78.89	95.42	73.75	65.00
S6	100.00	90.83	73.33	71.25	78.75	85.00
S7	97.08	100.00	82.92	90.42	70.00	59.58
S8	100.00	100.00	66.25	64.58	82.92	93.81
S9	97.92	94.17	62.50	77.50	57.08	77.08
S10	99.17	90.00	83.33	95.24	56.67	78.33
S11	97.50	92.92	54.17	76.25	69.17	69.58
S12	97.92	100.00	67.50	78.75	65.42	67.50
S13	100.00	100.00	63.33	70.00	60.00	89.17
S14	95.42	99.58	59.17	73.75	62.92	79.17
S15	100.00	100.00	66.25	88.75	52.08	56.25
S16	100.00	99.58	59.67	80.00	62.50	65.83
S17	86.67	89.17	59.58	59.17	55.00	70.42
S18	100.00	99.17	62.08	66.67	60.56	70.00
S19	100.00	99.58	61.25	75.00	65.83	71.25
S20	98.33	99.17	64.58	71.67	68.75	71.25
S21	97.92	99.58	69.58	72.50	70.83	71.67
S22	98.75	99.17	72.50	75.42	53.86	67.78
Mean	**98.20**	**97.47**	**65.79**	**76.10**	**65.18**	**73.27**
Std	**5.80**	**9.17**	**8.18**	**9.47**	**8.11**	**9.72**
P	##		***		**	

##: No significance; **: 0.001<*P*<0.01; ***: *P*<0.001

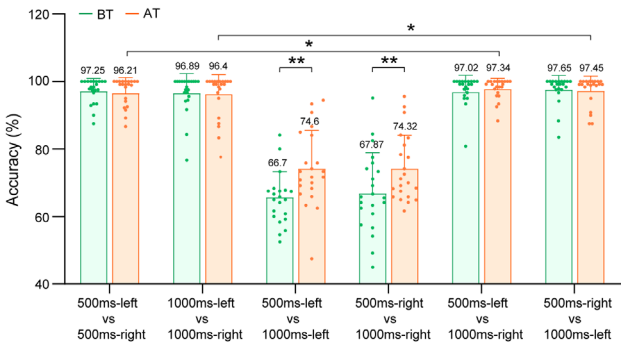

Fig. 7. Binary classification results between two pairs of movement-time dual intentions (500 ms-left, 500 ms-right, 1000 ms-left, 1000 ms-right) based on TS+LogR classification methods. *: 0.01<*P*<0.05; **: 0.001<*P*<0.01

To better understand how the involvement of precise timing prediction influences the decoding performance of dual intentions, this study investigated the binary classification in the BT and AT sessions, respectively. Fig. 7 shows average binary classification accuracies in BT and AT sessions. Significant improvement was found in the binary conditions of 500 ms-left vs. 1000 ms-left ($T(21)$=-3.089, P=0.006), and 500 ms-right vs. 1000 ms-right ($T(21)$=-3.045, P=0.006) after establishing precise timing prediction. These results indicated that the increase in AT sessions four-classification outcomes is primarily attributed to the heightened accuracy in recognizing time intention following the establishment of precise timing prediction.

In addition, the results also show that the feature differences between different time intentions (500 ms vs. 1000 ms) combined with the feature differences between different movement intentions (left vs. right) yielded higher classification accuracies (500 ms: $T(21)$=-2.123, P=0.046; 1000 ms: $T(21)$=-2.21, P=0.038) after precise timing prediction were established, further illustrating the close relationship between timing prediction and movement.

IV. DISCUSSION

This study designed a novel time-movement synchronous experiment that can simultaneously encode time and movement intentions, demonstrating a synergistic interaction pattern between precise timing prediction and movement. It also validated the hypothesis that a single EEG feature (20–60 Hz high-frequency power) can simultaneously decode time-movement dual intentions. Different from traditional BCIs where an EEG feature is used for detecting merely one intention, this study highlighted the new potential that two specific dimensions of information can be successfully decoded by using a single EEG feature. Such finding is promising to broaden the intentions detectable by active BCIs and provide new neurophysiological evidence for a deeper understanding of the neural mechanisms underlying the interaction between precise timing prediction and movement.

High-frequency (beta-gamma) power has a causal connection with timing prediction [32]. A decade ago, research revealed the brain's ability to internalize the temporal regularity of isochronous sound via beta band power modulation [33]. With specific time courses, beta power and its lateralization characteristics tend to be instrumental in predicting the onset of the target stimulus in a rhythmic sequence [15], [34]. Subsequent findings showed beta-gamma power variations in multi-second (>1000 ms) single-interval timing, which has a dissociation mechanism from the rhythmic temporal prediction [30]. To be specific, in interval production tasks, higher beta power between the two key presses indexed longer produced durations, and the coupling strength between alpha phase and beta power was sensitive to time production precision [35], [36]. Beyond indicating subsequent behaviours, beta-gamma oscillation was involved in the time-related predictive coding. In particular, beta power participates in the active neural encoding of duration information or temporal structure; it can be modulated by previously perceived intervals and react to the surprise about sensory event timing, just as in other prediction processes that depend on prior knowledge and place more focus on prediction surprise [37], [38], [39], [40], [41], [42]. Furthermore, gamma oscillation is indispensable in predictive timing, serving as a mechanism that underlies the maintenance of duration information [37], [43]. In the current study, larger beta-gamma ERD in the frontal and motor brain areas was observed in AT sessions, along with a significant beta-gamma ERD difference between 500 ms and 1000 ms timing. These

results not only reaffirm the crucial role of beta-gamma power but also provide additional neural evidence for a better understanding of precise timing prediction. Few studies have investigated whether the specific beta-gamma EEG pattern is an innate talent of the brain or not. Previous observations were induced by either imprecise time estimation or merely post-training precise timing prediction, providing no clear explanation for the doubt. This study found that the trained beta-gamma ERD was enhanced, and the ERD difference between 500 ms and 1000 ms was significant only in AT sessions. Decoding results based on 20–60 Hz power found the classification accuracy between the 500 ms and 1000 ms conditions was only 65.79% in the BT session, which improved to 76.10% in AT sessions. This indicated that improved sub-second time perception needs proper training, and the enhanced beta-gamma ERD may underlie such perception improvement, deepening the traditional understanding of precise timing prediction. Additionally, compared to numerous multi-second studies, few studies tested whether beta-gamma power still plays a fundamental role in sub-second single-interval timing. Our results confirmed beta-gamma ERD can index the length of time duration even in sub-second (<1000 ms) timescales, especially in the frontal and motor brain areas.

This study confirmed the EEG separability of sub-second timing predictions with distinct lengths. Previous studies often focused on the neural representations of timing prediction, which is a grand-averaged result across subjects and trials. Few studies explore the feasibility of detecting time intention based on the single-trial EEG data. For this, we conducted a sequence of studies to test the EEG separability induced by timing prediction with varied length. To be specific, in an interval matching task in visual modality, two temporal templates, 400 ms and 600 ms, were distinguished based on the combination feature of delta (0–4 Hz) waveform and beta-gamma (20–60 Hz) power, achieving 76.45% averaged binary classification accuracy [17]. In a duration production task, EEG features induced by 1000 ms, 1500 ms and 2000 ms timing predictions were analyzed, revealing a positive correlation between duration length and beta-gamma (20–60 Hz) ERD, with a 70.26% averaged tri-classification accuracy [31]. Even in a rhythmic tapping task, the time-related beta-gamma power variation was evident and decodable [44]. While these studies demonstrated the widespread involvement of beta-gamma ERD in the predictive timing process across various mental task, stimulus modality and duration length, a major drawback was the unchanged predicted temporal length within a single block, potentially strengthening neural representations of predictive timing with specific length. It needs exploring whether the high-frequency power distinctions induced by varied temporal length are still robust when there are several predicted temporal lengths within a single block. In the current study, the two predicted temporal lengths (500 ms vs. 1000 ms) randomly presented within a block. Remarkably, the beta-gamma power still differentiated the distinct temporal lengths, achieving 76.10% averaged time-related decoding accuracy (500 ms vs. 1000 ms) with a maximum accuracy of 95.42%, which provides strong evidence that the beta-gamma power is a robust EEG feature for detecting time intention.

The current study differed from other movement studies in two key aspects. Firstly, the time length required for representing movement intention is greatly reduced. Traditional motor imagery or motor execution paradigms usually need a time length of over 2 seconds to sufficiently express movement intention [45], [46], [47]; there also exists a long period that often exceeds 2 seconds for motor preparation [48]. However, this study completed motor execution almost instantaneously, with preparation times as short as 500 ms or 1000 ms. This rapid process raises questions about the effectiveness of movement detection under such conditions. The study revealed more negative pre-movement contralateral waveforms of motor-related cortical potential (MRCP) and pre-movement ERD lateralization in both the 500 ms and 1000 ms conditions, indicating that the motor-related EEG representations still exist even with extremely short movement expression times. Decoding results further showed that compared to the MRCP features in time domain, the power feature can provide more useful and stable information for decoding movement intention in the pre-movement period (supplementary A.5). Moreover, using the power feature with wider frequency band (20–60 Hz) achieved 98.20% and 97.40% average left-right classification accuracy, respectively, for the BT and AT sessions, which were much higher than using the power in a traditionally motor-related frequency band (20–30 Hz) (supplementary A.6).

Secondly, the involvement of timing prediction contributes to the evident difference from traditional movement studies that typically focus on a single intention in the subject's mind [49]. This dual encoding stressed an urgent need to explore the interactions between movement and timing prediction, a critical aspect for advancing active BCIs. To comprehend these intentions, the central concern is whether the EEG features of the two intentions can both remain robust enough for effective decoding, especially when one intention is enhanced. Timing prediction and movement are believed to have shared neural structures or circuits, such as the premotor cortex, inferior parietal lobule and the central thalamus [21], [50], [51]. Some studies found movement can promote the precision of timing prediction. For instance, a tone interval bias judgment task under auditory-motor synchronized stimulation reported a positive correlation between active motor control and P300 amplitude [12], as well as pre-stimulus beta power [52]. A syllable-tracking task for different frequencies found that combining rhythmic finger-tapping movements produced a more pronounced delta-beta coupling effect [53]. Recent studies on the impact of timing prediction on movement have started to unfold. Studies have shown that estimating longer time intervals would take up more cognitive resources. For example, a time estimation of 3000 ms can lead to the disappearance of potentials related to motor preparation when performing a motor task afterward [54]. However, other research on time perception reported that estimating durations shorter than 2000 ms tend to be automatic process that does not require taking up too much cognitive resources [6]. For

instance, in active motor control tasks based on temporal predictions within 1500 ms, a significant P3 component is observed under high-probability expectation conditions, reflecting the accumulation of motor resources [55]. Additionally, involvement in rhythmic temporal prediction within 1500 ms helps enhance the encoding and decoding of motor-related EEG signals [44]. However, these results primarily focused on the neural activities of either movement or timing prediction, with no study sufficiently describing the bidirectional interactions that equally consider EEG features induced by both intentions within an experiment, making it difficult to meet the demand of active BCIs to detect the time-movement dual intention. In this study, the 500 ms and 1000 ms timing predictions yielded more significant high-frequency (30–60 Hz) ERD difference in AT sessions, as well as a 10.31% improvement decoding accuracy. As the enhancement of timing prediction, larger lateralization of low-frequency MRCP and beta ERD was found, and the movement decoding accuracy remains nearly constant (P=0.37), which indicated the movement intention can still be robust when the timing prediction is enhanced. The results provide new neural evidence for better understanding the interactions between time and movement. Furthermore, this study concurrently detected time-movement dual intention based on the high-frequency (20–60 Hz) power, yielding a 73.27% average four-classification accuracy. The above results provide the first evidence that a single EEG feature can represent two mental processing.

The results of this study provide new perspectives and directions for further research on BCIs in the fields of neural control and motor rehabilitation. Firstly, in terms of enhancing the performance of BCIs in controlling external devices, this study clarifies the synergistic patterns between time and movement by thoroughly analyzing the EEG features related to these parameters, achieving a composite intention decoding based on single-subject, single-trial data. Building on this, future research could focus on the online decoding of time-movement composite intentions, which could improve the speed of conveying movement intention to various external devices, such as robotic arms, unmanned vehicles, and drones, as well as supporting the control of more complex information, thus realising the synergistic perception of time and movement by external devices. Also, it is necessary to expand the temporal command set by adding timing predictions, as the current duration and number of decodable commands are limited.

Secondly, in terms of enhancing the application of BCIs in motor rehabilitation, this study accelerated the information transmission rate of movement intention decoding and supported a broader range of cognitive content. This effectively prevents patients from experiencing fatigue or losing interest due to prolonged experimental sessions, thereby opening up new possibilities for developing innovative rehabilitation training models based on movement intention. A potential limitation of this study is that the task requires participants to perform a button press after completing the timing, which may restrict participation by individuals with motor impairments. To address this, future research could gradually transition from actual movement to motor imagery. Previous studies have shown that rhythmic temporal prediction significantly enhances both actual movement and motor imagery. By gradually introducing this transition in motor patterns, it may be possible to develop a new paradigm of motor imagery based on timing prediction in future studies.

VI. Conclusion

This study demonstrated that the neural representations of movement can remain robust even when the brain concurrently encodes the very precise single-interval timing prediction, providing new neural evidence for the interactions between time and movement. Moreover, for the first time, a single EEG feature, i.e., high-frequency (20–60 Hz) power, was verified effective in reflecting dual intentions of time and movement, which is a completely new approach for broadening the detectable intention and information dimension for the active BCIs.

References

[1] Y. Wang, M. Nakanishi, and D. Zhang, “EEG-Based Brain-Computer Interfaces,” Adv Exp Med Biol, vol. 1101, pp. 41-65, 2019.

[2] K. Värbu, N. Muhammad, and Y. Muhammad, “Past, Present, and Future of EEG-Based BCI Applications,” Sensors (Basel), vol. 22, no. 9, p. 44, Apr. 26 2022.

[3] T. O. Zander, C. Kothe , S. Jatzev, “Enhancing Human-Computer Interaction with Input from Active and Passive Brain-Computer Interfaces,” Springer London, pp. 181-99, 2010.

[4] J. Luo, Z. R. Feng, and N. Lu, “Spatio-temporal discrepancy feature for classification of motor imageries,” Biomedical Signal Processing and Control, vol. 47, pp. 137-144, Jan, 2019.

[5] K. Wang, M. P. Xu, Y. J. Wang, S. S. Zhang, L. Chen, and D. Ming, “Enhance decoding of pre-movement EEG patterns for brain-computer interfaces,” Journal of Neural Engineering, vol. 17, no. 1, Feb, 2020.

[6] C. V. Buhusi, W. H. Meck “What makes us tick? Functional and neural mechanisms of interval timing,” Nature reviews, vol. 6, no. 10, pp. 755-765, Oct, 2005.

[7] J. Coull, and A. Nobre, “Dissociating explicit timing from temporal expectation with fMRI,” Curr Opin Neurobiol, vol. 18, no. 2, pp. 137-44, Apr, 2008.

[8] A. C. Nobre, and F. van Ede, “Anticipated moments: temporal structure in attention,” Nat Rev Neurosci, vol. 19, no. 1, pp. 34-48, Jan, 2018.

[9] P. Hickey, H. Merseal, A. D. Patel, and E. Race, “Memory in time: Neural tracking of low-frequency rhythm dynamically modulates memory formation,” Neuroimage, vol. 213, pp. 116693, Jun, 2020.

[10] F. L. Bouwer, H. Honing, and H. A. Slagter, “Beat-based and Memory-based Temporal Expectations in Rhythm: Similar Perceptual Effects, Different Underlying Mechanisms,” J. Cogn. Neurosci., vol. 32, no. 7, pp. 1221–1241, Jul. 2020.

[11] M. Xu, J. Meng, H. Yu, T. P. Jung, and D. Ming, “Dynamic Brain Responses Modulated by Precise Timing Prediction in an Opposing Process,” Neurosci Bull, vol. 37, no. 1, pp. 70-80, Jan, 2021.

[12] N. Conradi, C. Abel, S. Frisch, C. A. Kell, J. Kaiser, and M. Schmidt-Kassow, “Actively but not passively synchronized motor activity amplifies predictive timing,” Neuroimage, vol. 139, pp. 211-217, Oct 1, 2016.

[13] A. P. Pinheiro, M. Schwartze, F. Gutierrez, and S. A. Kotz, “When temporal prediction errs: ERP responses to delayed action-feedback onset,” Neuropsychologia, vol. 134, Nov, 2019.

[14] Y. F. Hsu, J. A. Hämäläinen, and F. Waszak, “Temporal expectation and spectral expectation operate in distinct fashion on neuronal populations,” Neuropsychologia, vol. 51, no. 13, pp. 2548-2555, Nov, 2013.

[15] L. H. Arnal, K. B. Doelling, and D. Poeppel, “Delta-Beta Coupled Oscillations Underlie Temporal Prediction Accuracy,” Cerebral Cortex, vol. 25, no. 9, pp. 3077-3085, Sep, 2015.

[16] L. Grabot, T. W. Kononowicz, T. Dupré la Tour, A. Gramfort, V. Doyère, and V. van Wassenhove, “The Strength of Alpha-Beta Oscillatory

Coupling Predicts Motor Timing Precision," J. Neurosci., vol. 39, no. 17, pp. 3277–3291, Apr. 24 2019.

[17] J. Meng, M. Xu, K. Wang, Q. Meng, J. Han, X. Xiao, et al., "Separable EEG Features Induced by Timing Prediction for Active Brain-Computer Interfaces," Sensors (Basel), vol. 20, no. 12, p. 15, Jun. 25 2020.

[18] J. Meng, X. Li, Y. Zhao, R. Li, M. Xu, and D. Ming, "Modality-Attention Promotes the Neural Effects of Precise Timing Prediction in Early Sensory Processing," Brain Sci., vol. 13, no. 4, p. 16, Apr. 3 2023.

[19] M. Tanaka, J. Kunimatsu, T. W. Suzuki, M. Kameda, S. Ohmae, A. Uematsu, and R. Takeya, "Roles of the Cerebellum in Motor Preparation and Prediction of Timing," Neuroscience, vol. 462, pp. 220-234, May 10, 2021.

[20] A. Guillot, S. Daligault, D. Schwartz, and F. Di Rienzo, "Timing-specific patterns of cerebral activations during motor imagery: A case study of the expert brain signature," Brain and Cognition, vol. 167, Apr, 2023.

[21] K. Matsuyama, and M. Tanaka, "Temporal Prediction Signals for Periodic Sensory Events in the Primate Central Thalamus," Journal of Neuroscience, vol. 41, no. 9, pp. 1917-1927, Mar 3, 2021.

[22] E. Graber, and T. Fujioka, "Induced Beta Power Modulations during Isochronous Auditory Beats Reflect Intentional Anticipation before Gradual Tempo Changes," Scientific Reports, vol. 10, no. 1, Mar 6, 2020.

[23] R. E. London, C. S. Y. Benwell, R. Cecere, M. Quak, G. Thut, and D. Talsma, "EEG alpha power predicts the temporal sensitivity of multisensory perception," European Journal of Neuroscience, vol. 55, no. 11-12, pp. 3241-3255, Jun, 2022.

[24] S. Jun, J. S. Kim, and C. K. Chung, "Prediction of Successful Memory Encoding Based on Lateral Temporal Cortical Gamma Power," Frontiers in Neuroscience, vol. 15, May 25, 2021.

[25] R. Takeya, M. Kameda, A. D. Patel, and M. Tanaka, "Predictive and tempo-flexible synchronization to a visual metronome in monkeys," Scientific Reports, vol. 7, Jul 21, 2017.

[26] R. L. van den Brink, P. R. Murphy, K. Desender, N. de Ru, and S. Nieuwenhuis, "Temporal Expectation Hastens Decision Onset But Does Not Affect Evidence Quality," J. Neurosci., vol. 41, no. 1, pp. 130–143, Jan. 6 2021.

[27] A. D. Patel, and J. R. Iversen, "The evolutionary neuroscience of musical beat perception: the Action Simulation for Auditory Prediction (ASAP) hypothesis," Front Syst Neurosci, vol. 8, pp. 57, 2014.

[28] M. Stanczyk, E. Szelag, K. Krystecka, and A. Szymaszek, "A common timing mechanism across different millisecond domains: evidence from perceptual and motor tasks," Scientific Reports, vol. 13, no. 1, Nov 30, 2023.

[29] J. Samaha, P. Bauer, S. Cimaroli, and B. R. Postle, "Correction for Samaha et al., Top-down control of the phase of alpha-band oscillations as a mechanism for temporal prediction," Proc. Natl. Acad. Sci. USA, vol. 112, no. 46, pp. E6410–E6410, Nov. 17 2015.

[30] A. Breska, and R. B. Ivry, "Double dissociation of single-interval and rhythmic temporal prediction in cerebellar degeneration and Parkinson's disease," Proceedings of the National Academy of Sciences of the United States of America, vol. 115, no. 48, pp. 12283-12288, Nov 27, 2018.

[31] J. M. Author, "The Neural Representation, Mechanism, Coding and Decoding Methods of Predictive Temporal Template in Brain-Computer Interfaces," Ph.D. dissertation, Abbrev. Tianjin Univ, Tianjin, 2020.

[32] R. Bartolo, L. Prado, and H. Merchant, "Information Processing in the Primate Basal Ganglia during Sensory-Guided and Internally Driven Rhythmic Tapping," Journal of Neuroscience, vol. 34, no. 11, pp. 3910-3923, Mar 12, 2014.

[33] T. Fujioka, L. J. Trainor, E. W. Large, and B. Ross, "Internalized Timing of Isochronous Sounds Is Represented in Neuromagnetic Beta Oscillations," Journal of Neuroscience, vol. 32, no. 5, pp. 1791-1802, Feb 1, 2012.

[34] S. G. Heideman, F. van Ede, and A. C. Nobre, "Temporal alignment of anticipatory motor cortical beta lateralisation in hidden visual-motor sequences," European Journal of Neuroscience, vol. 48, no. 8, pp. 2684-2695, Oct, 2018.

[35] T. W. Kononowicz, and H. van Rijn, "Single trial beta oscillations index time estimation," Neuropsychologia, vol. 75, pp. 381-389, Aug, 2015.

[36] T. W. Kononowicz, T. Sander, H. Van Rijn, and V. van Wassenhove, "Precision Timing with α-β Oscillatory Coupling: Stopwatch or Motor Control?" J. Cogn. Neurosci., vol. 32, no. 9, pp. 1624–1636, Sep. 2020.

[37] S. Kulashekhar, J. Pekkola, J. M. Palva, and S. Palva, "The Role of Cortical Beta Oscillations in Time Estimation," Human Brain Mapping, vol. 37, no. 9, pp. 3262-3281, Sep, 2016.

[38] T. W. Kononowicz, C. Roger, and V. van Wassenhove, "Temporal Metacognition as the Decoding of Self-Generated Brain Dynamics," Cereb. Cortex, vol. 29, no. 10, pp. 4366–4380, Sep. 13 2019.

[39] V. Betti, S. Della Penna, F. de Pasquale, and M. Corbetta, "Spontaneous Beta Band Rhythms in the Predictive Coding of Natural Stimuli," Neuroscientist, vol. 27, no. 2, pp. 184-201, Apr, 2021.

[40] A. Damsma, N. Schlichting, and H. van Rijn, "Temporal Context Actively Shapes EEG Signatures of Time Perception," J. Neurosci., vol. 41, no. 20, pp. 4514–4523, May 19 2021.

[41] T. Meindertsma, N. A. Kloosterman, A. K. Engel, E. J. Wagenmakers, and T. H. Donner, "Surprise About Sensory Event Timing Drives Cortical Transients in the Beta Frequency Band," J. Neurosci., vol. 38, no. 35, pp. 7600–7610, Aug. 29 2018.

[42] J. Y. Meng, W. Yao, Q. F. Meng, X. Y. Li, H. Wang, M. P. Xu, et al., "Typical Neural Representations of Predictive Coding in Visual and Auditory Sensory Processing," Prog Biochem Biophys, vol. 50, no. 7, pp. 1501–1516, Jul. 2023.

[43] M. Salgado-Ménez, M. Espinoza-Monroy, A. M. Malagón, K. Mercado, and V. Lafuente, "Estimating Time and Rhythm by Predicting External Stimuli," Adv. Exp. Med. Biol., vol. 1455, pp. 159–169, 2024.

[44] J. Meng, Y. Zhao, K. Wang, J. Sun, W. Yi, F. Xu, et al., "Rhythmic temporal prediction enhances neural representations of movement intention for brain-computer interface," J. Neural Eng., vol. 20, no. 6, p. 14, Nov. 10 2023.

[45] M. Miri, V. Abootalebi, H. Saeedi-Sourck, D. Van De Ville, and H. Behjat, "Spectral representation of EEG data using learned graphs with application to motor imagery decoding," Biomed. Signal Process. Control, vol. 87, Jan, p. 105537, 2024.

[46] P. F. G. D. Vazquez, C. A. Stefano Filho, G. C. D. Melo, A. Forner-Cordero, and G. Castellano, "Reproducibility analysis of functional connectivity measures for application in motor imagery BCIs," Biomed. Signal Process. Control, vol. 85, Aug, p. 105061, 2023.

[47] V. K. Benzy, A. P. Vinod, R. Subasree, S. Alladi, and K. Raghavendra, "Motor Imagery Hand Movement Direction Decoding Using Brain Computer Interface to Aid Stroke Recovery and Rehabilitation," IEEE Trans. Neural Syst. Rehabil. Eng., vol. 28, no. 12, pp. 3051–3062, Dec. 2020.

[48] T. W. Kononowicz, T. Sander, and H. van Rijn, "Neuroelectromagnetic signatures of the reproduction of supra-second durations," Neuropsychologia, vol. 75, pp. 201-213, Aug, 2015.

[49] D. F. Xu, and Q. N. Wang, "Noninvasive Human-Prosthesis Interfaces for Locomotion Intent Recognition: A Review," Cyborg and Bionic Systems, vol. 2021, 2021.

[50] B. Nandi, A. Ostrand, V. Johnson, T. J. Ford, A. Gazzaley, and T. P. Zanto, "Musical Training Facilitates Exogenous Temporal Attention via Delta Phase Entrainment within a Sensorimotor Network," Journal of Neuroscience, vol. 43, no. 18, pp. 3365-3378, May 3, 2023.

[51] R. Yewbrey, M. Mantziara, and K. Kornysheva, "Cortical Patterns Shift from Sequence Feature Separation during Planning to Integration during Motor Execution," J. Neurosci., vol. 43, no. 10, pp. 1742–1756, Mar. 8 2023.

[52] M. Schmidt-Kassow, T. N. White, C. Abel, and J. Kaiser, "Pre-stimulus beta power varies as a function of auditory-motor synchronization and temporal predictability," Frontiers in Neuroscience, vol. 17, Mar 8, 2023.

[53] B. Morillon, and S. Baillet, "Motor origin of temporal predictions in auditory attention," Proceedings of the National Academy of Sciences of the United States of America, vol. 114, no. 42, pp. E8913-E8921, Oct 17, 2017.

[54] L. Zhang, H. Ren, R. Zhang, M. Chen, R. Li, L. Shi, D. Yao, J. Gao, and Y. Hu, "Time-estimation process could cause the disappearence of readiness potential," *Cogn Neurodyn,* vol. 16, no. 5, pp. 1003-1011, Oct, 2022.

[55] G. M. Duma, Granziol, U., Mento, G, "Should I stay or should I go? How local-global implicit temporal expectancy shapes proactive motor control: An hdEEG study," NeuroImage, vol. 220, Oct, 2020.